AIP | The Journal of Chemical Physics

Inhomogeneous charge transfer within monolayer zinc phthalocyanine absorbed on TiO2(110)

Shun Yu, Sareh Ahmadi, Chenghua Sun, Pooya Tabib Zadeh Adibi, Winnie Chow, Annette Pietzsch, and Mats Göthelid

Citation: The Journal of Chemical Physics **136**, 154703 (2012); doi: 10.1063/1.3699072
View online: http://dx.doi.org/10.1063/1.3699072
View Table of Contents: http://scitation.aip.org/content/aip/journal/jcp/136/15?ver=pdfcov
Published by the AIP Publishing

Inhomogeneous charge transfer within monolayer zinc phthalocyanine absorbed on TiO_2(110)

Shun Yu,[1,a)] Sareh Ahmadi,[1] Chenghua Sun,[2] Pooya Tabib Zadeh Adibi,[1] Winnie Chow,[1] Annette Pietzsch,[3] and Mats Göthelid[1,a)]
[1]*Materials Physics, ICT, Royal Institute of Technology, Electrum 229, SE-16440 Stockholm, Sweden*
[2]*The University of Queensland, ARC Centre of Excellence for Functional Nanomaterials and Centre for Computational Molecular Science, Australia Institute for Bioengineering and Nanotechnology, The University of Queensland, Qld 4072, Australia*
[3]*Max-lab, Lund University, Box 118, SE- 22100 Lund, Sweden*

(Received 28 July 2011; accepted 14 March 2012; published online 17 April 2012)

The d-orbital contribution from the transition metal centers of phthalocyanine brings difficulties to understand the role of the organic ligands and their molecular frontier orbitals when it adsorbs on oxide surfaces. Here we use zinc phthalocyanine (ZnPc)/TiO_2(110) as a model system where the zinc d-orbitals are located deep below the organic orbitals leaving room for a detailed study of the interaction between the organic ligand and the substrate. A charge depletion from the highest occupied molecular orbital is observed, and a consequent shift of N1s and C1s to higher binding energy in photoelectron spectroscopy (PES). A detailed comparison of peak shifts in PES and near-edge X-ray absorption fine structure spectroscopy illustrates a slightly uneven charge distribution within the molecular plane and an inhomogeneous charge transfer screening between the center and periphery of the organic ligand: faster in the periphery and slower at the center, which is different from other metal phthalocyanine, e.g., FePc/TiO_2. Our results indicate that the metal center can substantially influence the electronic properties of the organic ligand at the interface by introducing an additional charge transfer channel to the inner molecular part. © *2012 American Institute of Physics*. [http://dx.doi.org/10.1063/1.3699072]

INTRODUCTION

Phthalocyanines (Pc) are an important class of materials for applications in organic electronic devices by virtues of their good chemical and thermal stability, easy synthesis and especially tunable physical properties through decorating the organic center with a metal atom, metal-oxo, or metal-halide moiety.[1,2] Generally, device performance is not simply a summation of the properties of the different constituents, but can gain additional improvements or suffer from drawbacks from the interfacial structure.[3–5] Therefore, much efforts have been put into understanding the system of phthalocyanines on various substrates: semiconductors,[5] metals[6–8] and organic layers.[9–11] Meanwhile, scientists try to establish a "*universal rule*" for the interaction between organics, especially Pc, and semiconductor substrate based on theoretical calculations.[3,4]

In the past two decades, the oxide/organic interface, especially in the field of photovoltaics,[1,12] has attracted much interest. TiO_2 is usually used as the working electrode for such devices. Previously, we have found that Pc molecules (FePc,[13,14] TiOPc,[15] and H_2Pc (Ref. 16)) suffer from electron depletion when absorbed on TiO_2. However, the various contributions from the central parts to the organic ring are not yet clear, nor is the exact interaction of the organic part with the substrate. Zinc phthalocyanine (ZnPc, Figure 1) has been used as a model metal phthalocyanine[4,6,8] since the fully filled Zn d-orbital is deeply hidden below the organic ligand frontier orbitals. Thus the interaction between ZnPc and a surface is mainly mediated by the organic part.

In this work, we use photoelectron spectroscopy (PES) and near edge X-ray absorption fine structure spectroscopy (NEXAFS) to investigate the electronic structure of ZnPc during initial stages of growth on TiO_2. The analyses focus on the local charge distribution and charge transfer related screening, which are obtained by comparing PES peak shifts and NEXAFS resonant transitions' shifts. A slightly inhomogeneous charge density and a distinctively different charge transfer screening within the molecular plane are suggested at the interface, providing a model picture for the interaction between metal phthalocyanine organic ligands and TiO_2.

EXPERIMENTAL AND THEORETICAL METHODS

The experiment was done at the surface end station of beamline I511 at MAX-lab, Lund, Sweden. This beamline provides a horizontally polarized photon beam at grazing incidence (around 7°) in the soft X-ray region. A Scienta R4000 spectrometer is mounted on the analysis chamber, which can rotate around the axis of the photon beam. Sample preparation was done in the preparation chamber which is linearly connected to the analysis chamber and almost aligned to the photon beam. The chamber is equipped with an Ar sputter gun, sample annealing and low energy electron diffraction (LEED) optics, as well as a molecule evaporator.

a)Authors to whom correspondence should be addressed. Electronic addresses: shuny@kth.se and gothelid@kth.se.

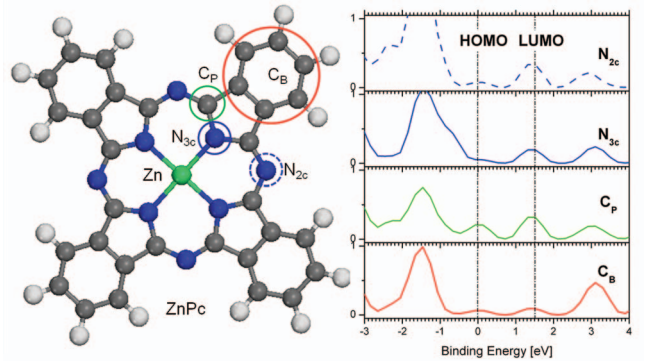

FIG. 1. Molecular structure of ZnPc (left) and average PDOS of a single atom (right). Pyrrole carbon and benzene carbon are marked as C_P (green circle) and C_B (red circle). Two coordinated and three coordinated nitrogen atoms are marked as N_{2c} (blue dashed circle) and N_{3c} (blue solid circle).

The substrate was a single crystal rutile TiO_2(110) (Surface Preparation Laboratory, the Netherlands) mounted with the [001] direction along the incident beam. After being introduced into the ultrahigh vacuum (UHV) chamber, the sample was thermally treated at around 1000 K in UHV to create oxygen vacancies and increase the conductivity. The sample color changed from transparent to light blue. Before each deposition, the surface was cleaned by several cycles of Ar^+ sputtering and annealing in UHV until the LEED showed a clear 1×1 pattern. ZnPc (Sigma-Aldrich, 97% purity) was deposited on the surface at room temperature by sublimation from a home-made Knudsen-type cell. The molecular powder was thoroughly outgassed before deposition, until no impurities (mainly water) were detected in mass-spectra.

Photoelectron spectra were collected after each deposition at normal emission. All spectra are normalized to the background: the intensity at the lower binding energy side for core levels and at 25 eV for valence band (VB) where neither substrate nor molecular orbitals contributes. Photoelectron spectra were collected using different photon energies and total energy resolutions: C1s 382 eV/117 meV, N1s 490 eV/150 meV, Zn3d/VB overview 160 eV/33 meV and VB gap region 80 eV/18 meV. To avoid beam damage, the sample was moved (1.7 μm/s) during X-ray exposure. The energy scale in PES was calibrated to the Fermi level, recorded from a tantalum foil in electrical contact with the substrate. Curve fitting of core level spectra was done with Voigt functions and a Shirley background by using the software Fitt-win.[17] The fitting parameters are listed in Table I. The coverage was determined by the ratio between the total N1s intensity and the maximum intensity of N1s interfacial component.

NEXAFS was measured in Auger yield mode. The spectrometer was placed in the plane perpendicular to the beam, and at 45° angle off the photon **E** vector plane. p and s polarization geometry were achieved by rotating the sample either normal or parallel to the **E** vector. The photon energy was calibrated from the difference in kinetic energy of the $Ti2p_{3/2}$ peak measured by the first and second order lights. C K-edge NEXAFS has been normalized to spectra collected from the clean TiO_2 surface at the corresponding polarization in order to remove contributions from carbon and chromium contaminations in the beamline optics.

TABLE I. Curve fitting parameters in Figure 2.

Coverage (ML)	C1s width (eV) GW[a]	LW (B)	LW (I,C_B)	LW (I,C_P)	N1s width (eV) GW	LW (B)	LW (I)
0.9	0.75	0.12	0.85	0.9	0.9	0.15	0.9
1.1	0.75	0.12	0.75	0.9	0.9	0.15	0.9
1.5	0.75	0.1	0.75	0.9	0.9	0.15	0.9
Thick	0.5	0.1	...	...	0.55	0.15	...

[a]GW: Gaussian width, LW (B): Lorentzian width of bulk like molecule, LW (I): Lorentzian width of interfacial state, and C_B, C_P: benzene carbon and pyrrole carbon.

Spin-polarized density functional theory (DFT) calculations have been carried out for a single molecule by using the DMol3 code.[18,19] We used the generalized gradient approximation (GGA) with the Perdew–Burke–Ernzerhof[20] functional (PBE) for the geometry optimization and the electronic structure calculations. Effective core potentials with double-numeric quality basis and all electron potentials with double-numeric polarized basis have been employed for the description of core electrons during the optimization and the energy calculation, respectively. In our calculations, the convergence criteria for structure optimizations were set to (a) energy tolerance of 1.0×10^{-6} Ha per atom, (b) maximum force tolerance of 1.0×10^{-4} Ha/Å, and (c) maximum displacement tolerance of 1.0×10^{-3} Å.

RESULTS AND DISCUSSION

Photoelectron spectroscopy

C1s and N1s core level spectra are arranged from bottom to top according to their coverages in Figure 2. In the top, typical phthalocyanine C1s (Figure 2(a)) and N1s (Figure 2(b)) spectra from the thick film are shown. C1s consists of three visible peaks at 284.7 eV, 286.1 eV and around 288.0 eV. The major one is assigned to benzene carbon (C_B as indicated in Figure 1), the second is due to pyrrole carbon (C_P) and the last one is the shake-up structure related to C_P.[21] The shake-up related to C_B, is located within the 2nd peak. The ratio between the pyrrole and benzene carbon contributions in PES depends on the surface sensitivity and molecular orientation.[22] For N1s, only one dominant peak appears at 398.8 eV, accompanied by a weak shake-up structure at 1.8 eV higher binding energy, which is close to the HOMO/LUMO gap.[23]

Spectra from films in the monolayer region display completely different line profiles. The dominant C1s feature is a peak around 285.4 eV with a shoulder at 284.6 eV and a broad hump centered at 287.5 eV. As the coverage increases, the shoulder at 284.6 eV gradually develops into the thick film spectrum while the dominant features from the monolayer are weakened. Similarly, N1s spectra (Figure 2(b)) contain a double peak in the monolayer region, instead of the single peak of the thick film, with the main component at 400.6 eV and the other at 398.9 eV. During the following depositions, the interface component vanishes and the spectrum develops into a bulk like spectrum.

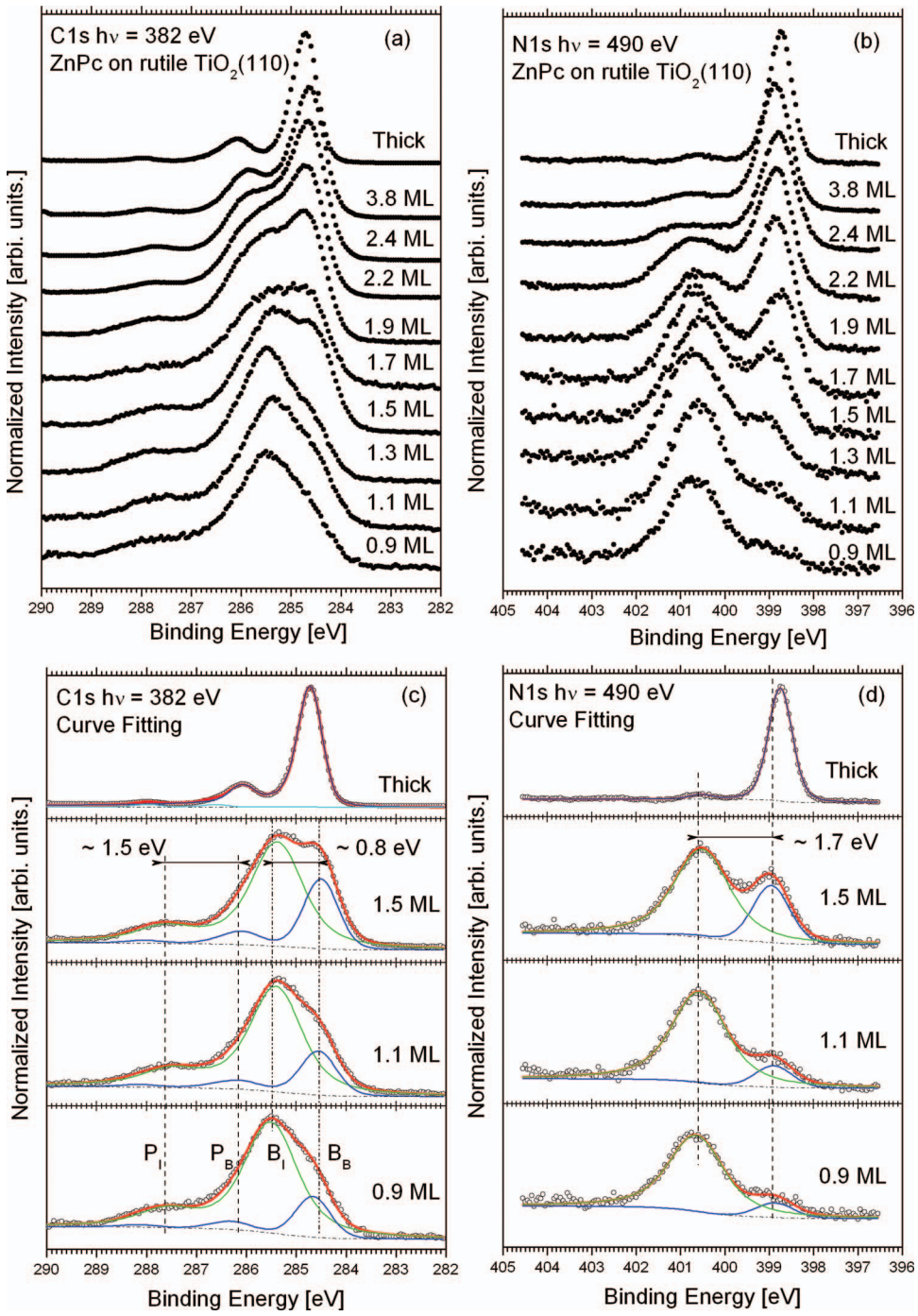

FIG. 2. Core level spectra of C1s (a) and N1s (b) from ZnPc on TiO_2. Curve fitting is done for C1s (c) and N1s (d) on selected coverages. P_I and B_I represent the pyrrole carbon and benzene carbon of interfacial molecules; P_B and B_B stand for the counterparts on bulk-like molecules. The energy shift is marked by dotted lines. In C1s (c), the shift between P_I and P_B is about 1.5 eV, while that of B_I and B_B is 0.8 eV. In N1s, the shift between interfacial molecules and bulk like molecule is around 1.7 eV.

We summarize the line profile development, 1) there are two different adsorption modes coexisting as deposited which display distinctive core level shifts; 2) the high binding energy components are assigned to interface molecules, indicating a strong influence from the substrate; the other features at lower binding energy are thus related to "bulk-like" molecules not in direct contact with the surface. It was also found that the intensity of the interfacial components did not saturate until the coverage reached 1.5 ML. Hence, initially this molecular film adopts an islands growth mode under our deposition condition.

Previously, Palmgren *et al.* reported a similar core level development for iron phthalocyanine (FePc) adsorbed on rutile TiO_2.[13] The shifts between interfacial and bulk-like molecules were: 1.2 eV for C_B, 1.1 eV for C_P and 1.3 eV for N1s.[13] In the present case, the C_B shift is considerably smaller than the N1s splitting. In order to extract the binding energy of each component, curve fitting was done. The results

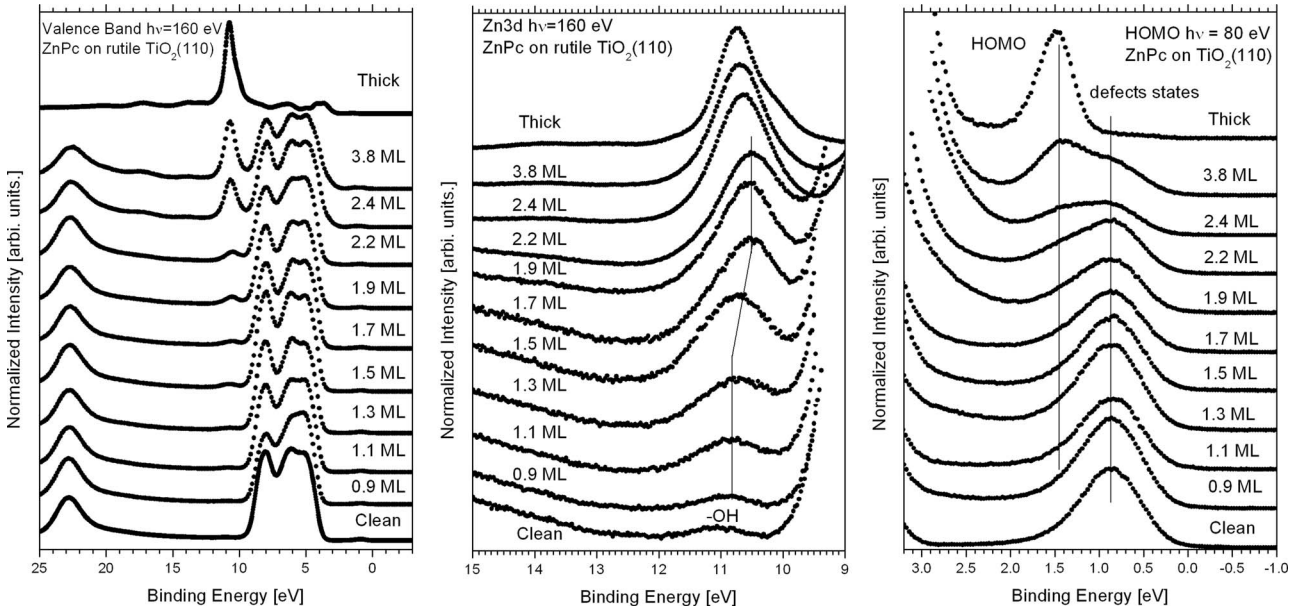

FIG. 3. Overview of valence band spectra (left), Zn3d spectra (middle) and HOMO region (right) at different coverages.

from selected preparations are presented in the lower panels of Figures 2(c) and 2(d). The fit is done with two different lines, each being a sum of separate Voigt functions (see table I for fitting parameters). The blue one represents the "unperturbed" bulk-like molecule and the green one represents interface molecules. We have used the same line profile and positions for all preparations. In Figure 2(c), C_B and C_P of the interfacial molecules (B_I, P_I) are shifted by approximately 0.8 eV and 1.5 eV to higher binding from the bulk-like components (B_B, P_B). Similar to FePc/TiO_2, no shake-up structure is observed for the interfacial components.[13] In Figure 2(d), the N1s shift between interfacial molecules and bulk-like molecules is about 1.7 eV.

The observed shifts (between interface molecules and "bulk-like" molecules) are the result of different electronic environments. The binding energy of the photoelectrons is determined by the combined initial state binding energy and the final state screening. From the initial state point of view, the chemical shift stems from the local charge distribution: the less charge surrounding the emitting atom, the higher the core level binding energy. In the final state, a poorer screening will shift the photoemission peak to higher binding energy, whereas a better screening will give an apparent lower binding energy.

According to the molecular structure of ZnPc (Figure 1), both C_P and nitrogen atoms are located in the inner part of the molecule while C_B is at the periphery. The N1s and C_P shifts are similar, 1.7 eV and 1.5 eV respectively, while the C_B shift is only 0.8 eV. Thus, the different shifts can be assumed to reflect differences in electronic environment on the inner and outer parts of the molecule. The chemical shift indicates electron deficiency all over the molecule. The larger core level shift on the inner atoms would also suggest that the central part has a lower charge density and/or is less screened than the outer part.

Since the spectral components overlap, especially C1s, one should take care not to over-interpret the fitting results. Nevertheless, a general tendency can be found for both C1s and N1s that the interfacial component has a larger Lorentzian width than the bulk component. Generally, the Lorentzian width is related to the life time of the core excited state: the larger the width is, the shorter the lifetime is. Thus, the core excited state of the interfacial molecules has a shorter life time than in the thick film.

Valence band spectra are shown in Figure 3. The thick film spectrum is plotted as a reference in the top of each panel. In the left panel, overview spectra show that molecular orbitals only slightly modify the substrate signals except of the rapid development of Zn3d orbital around 11 eV. In the middle panel, close-up spectra around the Zn3d region are presented. On the clean surface, a small hump is seen at 11.0 eV, which is due to the 3σ orbital of residual hydroxyl on the surface.[24] Zn3d appears at 10.8 eV at low coverage and shifts to 10.5 eV when 2 ML is achieved. Upon further deposition, the peak shifts back to higher binding energy and stays at 10.7 eV. Although we have not made any curve fitting, it is reasonable to assume at least two components within Zn3d: one from interfacial molecules at around 10.8 eV and the other from bulk-like molecules around 10.5 eV, following the discussion of C1s and N1s. The shift is much smaller than in N1s and C1s, but it was pointed out by theoretical calculations[25] that changing the molecular charge by either removing or adding electrons will have less influence on the charge around the Zn metal center, as it is moderated by the electron density of the periphery of Pc ring. Since Zn3d is filled and sufficiently deep to form almost pure molecular orbitals,[25,26] it is only mildly disturbed by charge transfer. Giovanelli *et al.*[27] have shown that Zn3d is well screened by the delocalized π electrons. In potassium doped ZnPc films it was shown that although the HOMO/LUMO shifted by 0.6 eV with respect to the Fermi level, Zn3d remained at the same position. In our case, the different shifts in Zn3d, C1s and N1s are a combined result of 1) the loss of electrons in the molecule mainly affects the inner ring of the molecule

and 2) the delocalized ligand orbitals efficiently screen the center Zn atom. Rienzo *et al.*[28] put zinc protoporphyrin on TiO_2, which has a similar molecular structure as ZnPc, and observed a removal of the zinc atom from the central porphyrin ring. This resulted in a Zn2p shift to lower binding energy compared the thick film, indicating a more neutral zinc atom on the surface. Their observation is opposite to ours, which excludes removal of zinc from the organic ring.

In the right panel of Figure 3, the HOMO region is displayed. A peak is observed around 0.9 eV on the clean surface which is the TiO_2 defects states.[24,29] The origin of this defect state is still under debate.[24,29] However, two possible types of defects may contribute to this state: the oxygen vacancies and interstitial Ti atoms. According to the simulation, adsorbing hydroxyl groups do not greatly influence this state.[30] Based on our previous study on the 4 tert-butyl pyridine on TiO_2, oxygen vacancies should still exist according to the similar sample preparation procedure.[31] At low coverage the molecular film does not display any HOMO structure, similar to FePc,[13] indicating that HOMO has a lower electron density for interfacial molecules, as previously suggested by the core level shifts and the absence of shake-up structure in the interfacial component. As the coverage increases, the HOMO gradually emerges at 1.4 eV aligned with the HOMO of the thick film. Meanwhile, the substrate defect state at 0.9 eV gradually decreases with increasing molecular coverage, but it is visible even at 2 ML coverage. A similar adsorption process has been found for other organic molecules.[29,32,33] It suggests that ZnPc does not prefer bonding to defects, contrary to 4-tert-butyl pyridine that preferentially binds to oxygen vacancies.[31,34]

Based on our theoretical calculations (Figure 1, right) and other simulation reports,[25,35] the HOMO of ZnPc is essentially the a_{1u} orbital with main contributions from pyrrole carbons, C_P. Hence, when charge is removed a larger charge deficiency may be expected for the inner ring. Even though nitrogen and zinc contribute less to HOMO, they are indirectly influenced by charge variations in the HOMO. However, upon electron depletion, the charge will be redistributed over the molecular plane,[25] which may in turn result in a homogeneous charge distribution. In addition, final state effects are critical; both VB development and core level shifts agree with the theoretically predicted charge transfer from Pc to TiO_2, where a strong orbital coupling was predicted.[3,4] Although calculations were made for p-type anatase TiO_2 and our sample is n-type rutile TiO_2(110), the orbital coupling is still possible. This will be discussed later.

At higher coverage there are several possible reasons for shifts in photoemission peaks. They can be of local character and of a more global character. The global ones are: charge transfer across the organic/TiO_2 interface leading to band bending shifts[36] and polarization screening from the substrate in the photoemission measurement, which exponentially decays with distance to the substrate.[37] In both cases one would expect shifts in the same direction and of (not exactly but) similar magnitude for all peaks. Typically when the screening is reduced, the shift goes to higher binding energy. In the present case, for bulk-like molecules which are not in direct contact with the surface, C_P and Zn3d shift to higher binding energy while N1s shifts oppositely and no observable shift for HOMO. The absence of systematic coverage dependent shifts cannot be satisfactorily explained by the above two global effects. Meanwhile, interfacial molecules experience a strong site-specific chemical shift. Thus, we suggest that the local electronic structure (initial state) and the local charge transfer screening plays a dominant role in this case, similar to that on metal surfaces.[38]

NEXAFS

We use NEXAFS to characterize the empty molecular orbitals. The results in Figure 4 were collected at the nitrogen K-edge under two different polarizations: p and s. In Figure 4(a), the spectra show a clear coverage dependence under p polarization. At the lowest coverage (bottom spectrum), only two principal transitions are observed: A´ at 399.4 eV which is assigned to transitions into the lowest unoccupied molecular orbital (LUMO) on molecules at the interface, C at 402.7 eV with a weak shoulder at 401.7 eV (D), is related to transitions into higher empty π^* orbitals.

After further deposition, a shoulder develops at lower photon energy and the spectra broaden. This shoulder continues to evolve into the dominant feature (A) at 398.7 eV at high coverage while A´ gradually vanishes. Thus A corresponds to the N1s $\rightarrow$ LUMO transition in bulk-like molecules. It is reasonable to expect that the N1s $\rightarrow$ LUMO transition of the interface molecules requires higher photon energy since the N1s of interface molecules is deeper than that of bulk-like molecules by 1.7 eV. However, the core level shift is not necessarily comparable to the NEXAFS shift since the final states might be quite different: the PES final state is a core ionized state with external screening while the NEXAFS final state is neutral with a core hole and an electron in an excited state.[39] NEXAFS peak B develops in a manner similar to peak A; it is missing at 0.9 ML but emerges with increasing coverage. Transition C at 402.6 eV is visible (under this polarization) at almost the same position for all preparations, i.e., the energy difference between N1s and the related empty orbital are similar for both interfacial and bulk-like molecules.

Under s polarization, the line profile develops differently with coverage as illustrated in Figure 4(b). At 0.9 ML, the resonant enhancements at A´ and D are visible (although vaguely), but C is barely seen. In addition, A and B, which are related to transitions within bulk-like molecules, are not visible until above 2 ML coverage. Since the π^* orbital are perpendicular to the molecular plane, the strongest transition from N1s to π^* should be achieved when the polarization is normal to the molecular plane; the lowest intensity occurs when **E** vector is parallel to the molecular plane. For the configuration of interfacial molecules (0.9 ML), the azimuthal dependence has to be taken into account due to the potentially preferential adsorption of molecule on the twofold symmetric TiO_2(110) surface, in which case the intensity of absorption peak is related with $\cos^2\phi$ (ϕ : azimuth angle).[40,41] The TiO_2(110) surface has bridge oxygen rows protruding out of the surface along [001] and five coordinated Ti row between.[29] Several previous results have found that

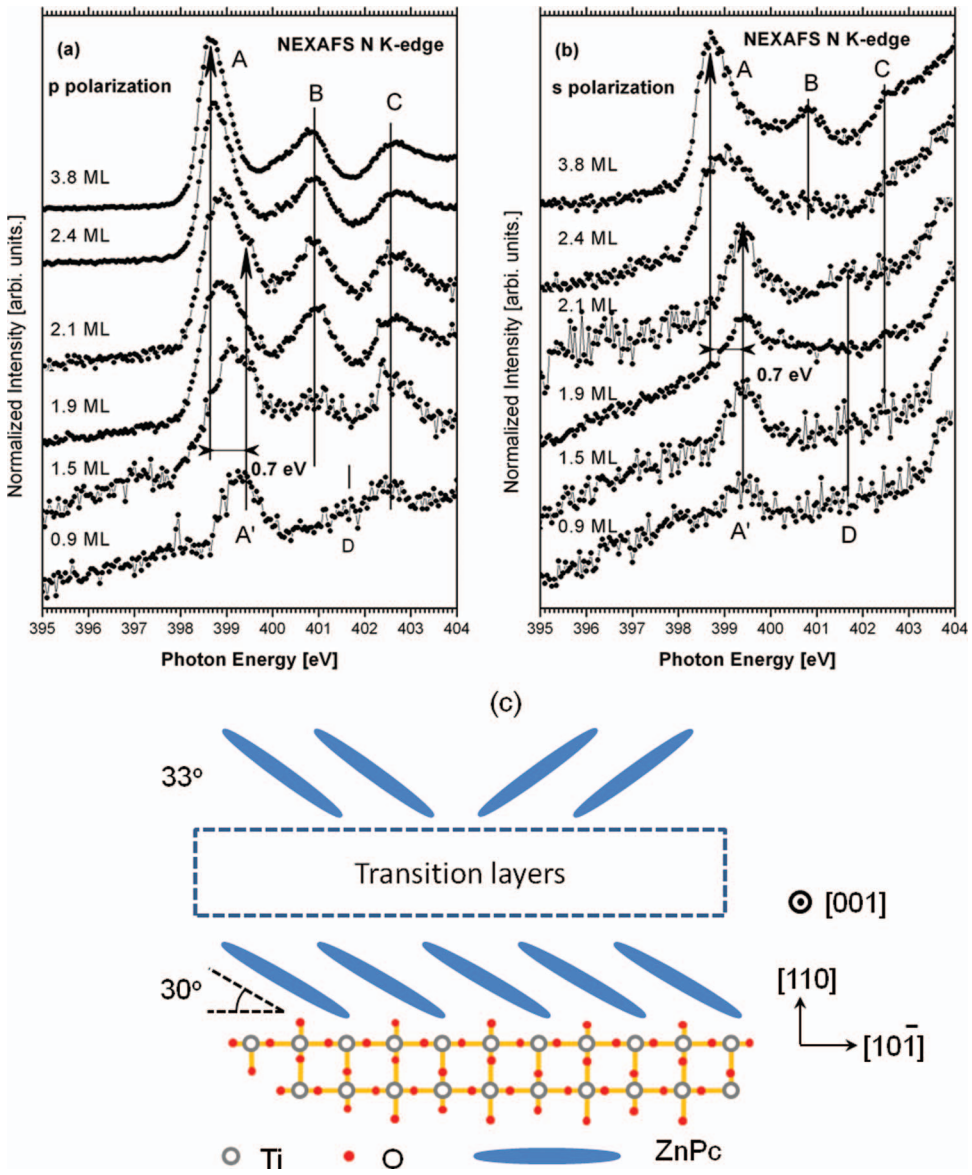

FIG. 4. N K-edge NEXAFS spectra at different coverages under p polarization (a) and s polarization (b). A and A′ denote the N1s → LUMO transitions of bulk-like molecules and interfacial molecules, respectively. Transition B and C of the bulk like molecule and transition D of the interfacial state molecule represent the ones from N1s to higher empty π^* orbitals. (c): the schematic of the molecular orientation ZnPc adsorbed on TiO_2(110). Ti is marked in grey circle; O is in red dot; blue ellipse represents the cross-section of ZnPc. The molecule is aligned along [001] direction which is perpendicular to the paper in the first layer. Horizontal orientation is [10-1] direction and vertical orientation is [110] direction. The interfacial molecules layer is estimated tilted on the surface at 30°; the thicker layer is packing at 33° under a free azimuthal assumption. In between, there are transition layers, which we cannot determine the angle.

aromatic organic molecules can align along [001][29,42–44] with the molecular plane parallel with [001]. If we apply this in our case, with a grazing incident beam along [001] and 7° off the surface plain, the molecular plane can be estimated to be tilted by about 30° from the surface (Figure 4(c)). Additionally, several reports have shown that when Pc are adsorbed on metal surfaces the molecular plane will experience distortion and deformation.[45–48] By using X-ray standing waves, Yamane *et al.*[46] reported that ZnPc is buckled on Cu(111), with the zinc center pulled towards the surface, and the carbon periphery also bending downwards compared to the central pyrrole nitrogen ring. Pre-fluorinated Pc ($ZnPcF_{16}$ and $CuPcF_{16}$) deform in the opposite direction on metal surfaces with the fluorine atoms facing the vacuum.[46–48] Thus, more theoretical and experimental work is needed to precisely determine the monolayer molecular configuration. At 3.8 ML, the line profiles in the π^* region from the two polarizations resemble each other and are also consistent with previously reported results for ZnPc.[22,49,50] One can estimate the molecular tilt angle to 33° by assuming a free azimuthal rotation because of the rather week interaction between the molecular layers (Figure 4(c)).[40,51,52]

All nitrogen atoms are in the inner part of the molecule, while carbon atoms are located both on the inner and outer parts of the molecular plane. We can use carbon K-edge NEXAFS to separate the information from inner and peripheral parts (Figure 5). The spectrum collected at 3.8 ML resembles spectra from other metal phthalocyanines.[53–55] In

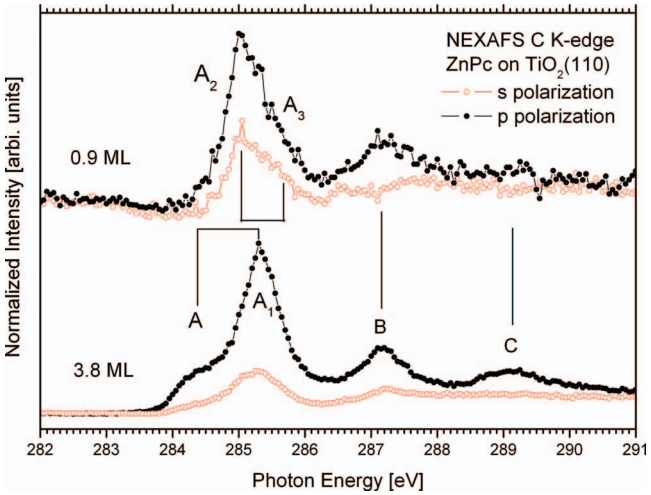

FIG. 5. C K-edge NEXAFS spectra from 0.9 ML (top) and 3.8 ML (bottom). Spectra collected under p and s polarization are plotted with black filled dotted line and red open dotted line. A and A_1 are transitions from C_B and C_P to LUMO for the bulk like molecule, while A_2 and A_3 are attributed to the C1s transitions to LUMO for interfacial molecules. Transition B and C stem from the excitation from C1s to higher empty π^* orbitals.

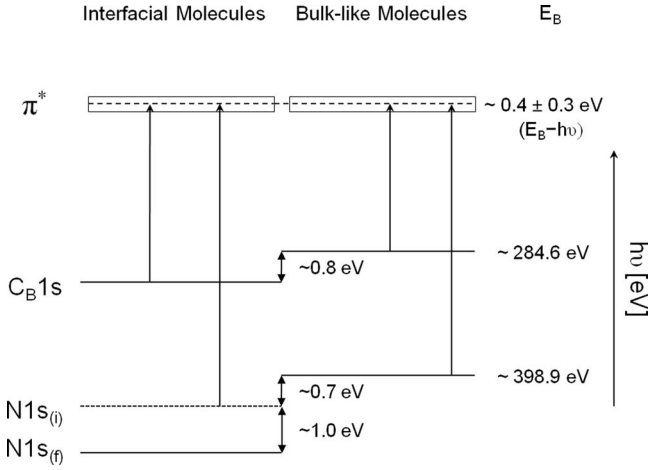

FIG. 6. The alignment of PES and NEXAFS for interfacial molecules (left) and bulk-like molecules (right). Single arrow represents the NEXAFS transition. Double arrow marks the core level differences. π^* is the lowest excited state for both case, the value is determined by subtracting the excitation energy ($h\upsilon$) in NEXAFS from the core level E_B. For C_B1s, the PES binding energy difference matches the photon energy difference in NEXAFS. For N1s, $N1s_{(i)}$ is the initial state while $N1s_{(f)}$ represents the contribution from the additional final state screening in PES. In NEXAFS, the external final screening is not influential and thus mainly the initial state is probed.

general, A (284.3 eV) and A_1 (285.3 eV) are ascribed to C_B and C_P 1s → LUMO transitions, respectively, and their separation was explained by the different C1s binding energies.[53,54] For a more detailed description, detailed theoretical calculations are needed.[56,57] At 0.9 ML, the well separated A and A_1 peaks are replaced by a single asymmetric peak A_2 at 285.0 eV with a shoulder A_3 around 285.6 eV. The A_2 – A separation is similar to the PES C_B separation between interfacial/bulk like molecules (0.8 eV), and we thus ascribe A_2 mainly to C_B → LUMO transitions in interface molecules, while A_3 is assigned to the transitions from C_P to LUMO. Transitions B and C are due to transitions from C1s to higher empty π^* orbitals. There are no shifts at 3.8 ML between s and p polarization, but the intensity of all peaks is weaker at s-polarization, in agreement with a tilted geometry suggested by N K-edge NEXAFS. At 0.9 ML, transition B remains at the same position in p-polarization but is split into two weak features in s-polarization. Transition C is vaguely observed in p-polarization and not observed at all in s-polarization. These rather different line profiles, including A, $A_{1,2,3}$, B and C, at low and high coverages indicate that distinctive molecular orbital symmetries, transition matrix and/or molecular configurations have been adopted by the interfacial state compared to the bulk state, also pointing to a potential orbital coupling at the interface.

The first NEXAFS resonance corresponds to a final state with an electron in the LUMO and a core hole.[40,58] While the photoemission final state usually be heavily influenced by different screening, The transition between core level and π^* orbital in NEXAFS is generally much less affected by the final state screening, since the system is self-screened, and thus the transition shift can be regarded to be mainly dependent on the initial state.[40,59] Core level photoemission is indistinguishable from NEXAFS only when the core hole is efficiently screened by electron transfer from the substrate to the unoccupied orbital.[40,58] Figure 6 compares initial and final state effects of PES and NEXAFS for both interface and bulk-like molecules. The PES binding energy (E_B) is according to Figure 2, while π^* is determined by the E_B-hυ from NEXAFS. The coincidence of the C_B1s chemical shift in PES and the A-A_2 NEXAFS shift indicates that the shift is mainly an initial state shift, due to different chemical environment. It also indicates that an efficient charge transfer screening channel exits in PES after removing a charge from system, the effect of which is comparable to that of the self-screening in NEXAFS. However, a larger discrepancy between the N1s chemical shift (1.7 eV) and the N NEXAFS shift (0.7 eV) is observed. For the same reason as above we assign the 0.7 eV to an initial state difference ($N1s_{(i)}$), while the additional ~1.0 eV shift is due to poorer external screening at the molecular pyrrole ring, which leads to the final state $N1s_{(f)}$. Hence, the different N1s and C_B1s chemical shifts on interfacial molecules is to a large extent due to a poorer screening on the inner ring than on the peripheral part, whereas the minor difference in NEXAFS shifts (0.7 eV N; 0.8 eV C_B) indicate only a slightly uneven charge distribution around the organic ligand. This was theoretically explained as the organic ligand moderates the extra charge.[25]

Our 0.9 ML C K-edge NEXAFS resembles those from heavily potassium doped Pc films.[60–62] In the case of doping, LUMO is filled by electrons from the dopant and will consequently influence the transition probability from core level to LUMO. In addition, a new doping induced C1s component appeared between C_P and C_B, and the first absorption peak was assigned to a transition between this state and LUMO.[61] Additionally, Kröger *et al.*[63] found that in the submonolayer region CuPc experienced a substrate-mediated charge transfer from HOMO and HOMO-1 to LUMO on Ag(111) in order to minimize the energy. This leads to the following question: is the donation of electrons from HOMO accompanied by a

back donation of electrons from the substrate into LUMO in our case?

Filling the LUMO usually gives additional photoemission intensity near the Fermi level,[27,63] which is not supported by our valence band results. Moreover, when doping the organic film the transition to higher π^* orbitals of both C and N K-edge (transition B and C) should shift to lower photon energy,[60–62] which is not the case here. Hence, we find no support for a back donation.

According to the analysis of NEXAFS and PES, interface molecules tilt on the surface, creating a channel for charge transfer. Upon adsorption, HOMO electrons transfer away from the molecule through this channel. The channel is also open for electron transfer in the opposite direction, for example following a core excitation. Due to the highly delocalized nature of the phthalocyanine π orbitals,[25] charge transfer from or to the substrate will be moderated within the whole molecular plane, leaving a rather even charge distribution. M.P. de Jong *et al.* reported that for Fe(II)-tetraphenylporphyrin (FeTTP) adsorbed on MoS_2, the phenyl group in the periphery experience a much faster charge transfer than the inner porphyrin part, even though the central Fe atom interacts with the substrate.[64] Taking the structural similarity between FeTTP and phthalocyanines into account, their results support our argument that a core excited benzene (phenyl) is better screened through charge transfer from the substrate than the pyrrole part. The smaller Lorentzian width on C_B than on C_P at the interface, indicates a longer core hole lifetime on C_B than on C_P which seems in conflict with the screening times. However, the core hole decay (Auger decay) takes place within the atom and can be much slower than that required to relax into a fully screen core-hole state.[65,66]

Earlier in the discussion, we mentioned that our previous work on FePc/TiO_2 showed rather homogeneous core level shifts on C_P, C_B and N1s by 1.2 ± 0.1 eV, which is apparently different from the present case. From comparison of NEXAFS shifts and PES shifts, we conclude that the discrepancy can be assigned to a poorer screening around the central organic ring in the ZnPc case. There are at least three aspects which may contribute to this scenario. Firstly, theoretical calculations[25,35] and experiments[7,8,64,67] predict and illustrate that the open shell Fe d−orbitals contribute to the HOMO and participate in the interaction with substrate or doping. However, the zinc metal center with filled d-orbitals is rather inert compared to Fe and less influenced by changes in the peripheral part of the molecule. Thus, Pc-substrate orbital hybridization through the central atom may generate different screening for interface molecules depending on the central atom. Secondly, the molecular tilt angle may influence the extent of orbital hybridization: for ZnPc it is about 30° which may block the direct contact between Zn and substrate; whereas, FePc has a smaller contact angle seen by STM,[13] facilitating the central atom − substrate orbital hybridization. Thirdly, theoretical calculations[25] show that the bond length between the Fe and N_{3c} (∼1.92 Å) is shorter than that between Zn and N_{3c} (∼1.98 Å), which may also intrinsically influence the screening. Thus, the metal center can greatly influence the electronic properties of the organic ligand by introducing additional charge transfer channel.

CONCLUSIONS

Detailed analyses on the adsorption of ZnPc on TiO_2 by PES and NEXAFS have been carried out. We observe a clear difference in terms of electronic structure between interface molecules in direct contact with the substrate and those not in contact with TiO_2. The interface molecules bind to the surface with the molecular plane 30° from the surface plane, whereas at higher coverage the molecules tilt at 33°. The growth is of island type at room temperature. In agreement with previous studies on Pc/TiO_2,[13–16] it is found that charge is transferred away from the molecular HOMO into the substrate. Further comparison between NEXAFS resonance shifts and PES shifts points to a considerable screening difference between molecular center and periphery. The different core level interface shifts between center and periphery of the organic ligand of ZnPc compared to FePc[13] is explained by the absence of the central metal related efficient charge transfer channel, showing the influence of metal atoms to the organic ligand.

ACKNOWLEDGMENTS

Authors would like to acknowledge Dr. Pål Palmgren (VG-Scienta AB) for fruitful discussions and support. The Max-lab staff is kindly acknowledged. The Swedish Energy Agency (STEM), the Swedish Research Council (VR), the Göran Gustafsson Foundation, the Carl Trygger Foundation and the Queensland government are kindly acknowledged for financial support. Computational resources used in this work were provided by the University of Queensland (Centre for Computational Molecular Science) and the Australian Research Council (LIEF grant LE0882357: A Computational Facility for Multiscale Modeling in Computational Bio and Nanotechnology).

[1] A. W. Hains, Z. Liang, M. A. Woodhouse, and B. A. Gregg, Chem. Rev. **110**, 6689–735 (2010).
[2] K. Y. Law, Chem. Rev. **93**, 449–486 (1993).
[3] G. Mattioli, F. Filippone, P. Giannozzi, R. Caminiti, and A. Amore Bonapasta, Phys. Rev. Lett. **101**, 126805 (2008).
[4] G. Mattioli, F. Filippone, P. Giannozzi, R. Caminiti, and A. Amore Bonapasta, Chem. Mater. **21**, 4555–4567 (2009).
[5] N. Papageorgiou, E. Salomon, T. Angot, J.-M. Layet, L. Giovanelli, and G. Le Lay, Prog. Surf. Sci. **77**, 139–170 (2004).
[6] M. Grobosch, V. Yu. Aristov, O. V. Molodtsova, C. Schmidt, B. P. Doyle, S. Nannarone, and M. Knupfer, J. Phys. Chem. C **113**, 13219–13222 (2009).
[7] P. Gargiani, A. Calabrese, C. Mariani, and M. G. Betti, J. Phys. Chem. C **114**, 12258–12264 (2010).
[8] P. Gargiani, M. Angelucci, C. Mariani, and M. G. Betti, Phys. Rev. B **81**, 085412 (2010).
[9] M. Häming, M. Greif, M. Wieβner, A. Schöll, and F. Reinert, Surf. Sci. **604**, 1619–1622 (2010).
[10] W. Chen, H. Huang, S. Chen, X. Y. Gao, and A. T. S. Wee, J. Phys. Chem. C **112**, 5036–5042 (2008).
[11] S. Yim, S. Heutz, and T. S. Jones, Phys. Rev. B **67**, 165308 (2003).
[12] A. Hagfeldt, G. Boschloo, L. Sun, L. Kloo, and H. Pettersson, Chem. Rev. **110**, 6595–663 (2010).
[13] P. Palmgren, K. Nilson, S. Yu, F. Hennies, T. Angot, C. I. Nlebedim, J.-M. Layet, G. Le Lay, and M. Göthelid, J. Phys. Chem. C **112**, 5972–5977 (2008).
[14] P. Palmgren, S. Yu, F. Hennies, K. Nilson, B. Åkermark, and M. Göthelid, J. Chem. Phys. **129**, 074707 (2008).
[15] S. Yu, S. Ahmadi, P. Palmgren, F. Hennies, M. Zuleta, and M. Göthelid, J. Phys. Chem. C **113**, 13765–13771 (2009).

[16]P. Palmgren, B. Priya, N. Niraj, and M. Göthelid, Solar Energy Mater. Solar Cells **90**, 3602–3613 (2006).
[17]"Fitt-win" is the Windows version of "Fitt," a free software developed by Hyun-Jo Kim, berd@escalab.snu.ac.kr (2000).
[18]B. Delley, J. Chem. Phys. **92**, 508 (1990).
[19]B. Delley, J. Chem. Phys. **113**, 7756 (2000).
[20]J. P. Perdew, K. Burke, and M. Ernzerhof, Phys. Rev. Lett. **77**, 3865–3868 (1996).
[21]B. Brena, Y. Luo, M. Nyberg, S. Carniato, K. Nilson, Y. Alfredsson, J. Åhlund, N. Mårtensson, H. Siegbahn, and C. Puglia, Phys. Rev. B **70**, 195214 (2004).
[22]L. Zhang, H. Peisert, I. Biswas, M. Knupfer, D. Batchelor, and T. Chassé, Surf. Sci. **596**, 98–107 (2005).
[23]U. Weiler, T. Mayer, W. Jaegermann, C. Kelting, D. Schlettwein, S. Makarov, and D. Wöhrle, J. Phys. Chem. B **108**, 19398–19403 (2004).
[24]S. Wendt, P. T. Sprunger, E. Lira, G. K. H. Madsen, Z. Li, J. Ø. Hansen, J. Matthiesen, A. Blekinge-Rasmussen, E. Lægsgaard, B. Hammer, and F. Besenbacher, Science **320**, 1755–9 (2009).
[25]M.-S. Liao and S. Scheiner, J. Chem. Phys. **114**, 9780 (2001).
[26]G. Ricciardi, A. Rosa, and E. J. Baerends, J. Phys. Chem. A **105**, 5242–5254 (2001).
[27]L. Giovanelli, P. Vilmercati, C. Castellarin-Cudia, J.-M. Themlin, L. Porte, and A. Goldoni, J. Chem. Phys. **126**, 044709 (2007).
[28]A. Rienzo, L. C. Mayor, G. Magnano, C. J. Satterley, E. Ataman, J. Schnadt, K. Schulte, and J. N. O'shea, J. Chem. Phys. **132**, 084703 (2010).
[29]U. Diebold, Surf. Sci. Rep. **48**, 53–229 (2003).
[30]C. D. Valentin, G. Pacchioni, and A. Selloni, Phys. Rev. Lett. **97**, 166803 (2006).
[31]S. Yu, S. Ahmadi, C. Sun, P. Palmgren, F. Hennies, M. Zuleta, and M. Göthelid, J. Phys. Chem. C **114**, 2315–2320 (2010).
[32]S. Yu, S. Ahmadi, M. Zuleta, H. Tian, K. Schulte, A. Pietzsch, F. Hennies, J. Weissenrieder, X. Yang, and M. Göthelid, J. Chem. Phys. **133**, 224704 (2010).
[33]L.-Q. Wang, A. N. Shultz, D. R. Baer, and M. H. Engelhard, J. Vac. Sci. Technol. A **14**, 1532–1538 (1996).
[34]M. Göthelid, S. Yu, S. Ahmadi, C. Sun, and M. Zuleta, Int. J. Photoenergy **2011**, 1–6 (2011).
[35]I. Bruder, J. Schöneboom, R. Dinnebier, A. Ojala, S. Schäfer, R. Sens, P. Erk, and J. Weis, Org. Electron. **11**, 377–387 (2010).
[36]E. M. J. Johansson, M. Odelius, P. G. Karlsson, H. Siegbahn, A. Sandell, and H. Rensmo, J. Chem. Phys. **128**, 184709 (2008).
[37]H. Peisert, M. Knupfer, T. Schwieger, J. M. Auerhammer, M. S. Golden, and J. Fink, J. Appl. Phys. **91**, 4872 (2002).
[38]H. Peisert, A. Petershans, and T. Chassé, J. Phys. Chem. C **112**, 5703–5706 (2008).
[39]P. A. Brühwiler, O. Karis, and N. Mårtensson, Rev. Mod. Phys. **74**, 703–740 (2002).
[40]J. Stöhr, *NEXAFS Spectroscopy* (Springer-Verlag, Berlin, 1992).
[41]J. Stöhr and D. A. Outka, Phys. Rev. B **36**, 7895 (1987).
[42]V. Lanzilotto, C. Sanchez-Sanchez, G. Bavdek, D. Cvetko, M. F. Lopez, J. A. Martin-Gago, and L. Floreano, J. Phys. Chem. C **2**, 110224123313029 (2011).
[43]Y. Wang, Y. Ye, and K. Wu, J. Phys. Chem. B **110**, 17960–5 (2006).
[44]S. Godlewski, A. Tekiel, J. Budzioch, A. Gourdon, J. S. Prauzner-Bechcicki, and M. Szymonski, ChemPhysChem **10**, 3278–84 (2009).
[45]J. D. Baran, J. A. Larsson, R. A. J. Woolley, Y. Cong, P. J. Moriarty, A. A. Cafolla, K. Schulte, and V. R. Dhanak, Phys. Rev. B **81**, 075413 (2010).
[46]H. Yamane, A. Gerlach, S. Duhm, Y. Tanaka, T. Hosokai, Y. Y. Mi, J. Zegenhagen, N. Koch, K. Seki, and F. Schreiber, Phys. Rev. Lett. **105**, 046103 (2010).
[47]H. Peisert, D. Kolacyak, and T. Chassé, J. Phys. Chem. C **113**, 19244–19250 (2009).
[48]A. Gerlach, F. Schreiber, S. Sellner, H. Dosch, I. A. Vartanyants, B. C. C. Cowie, T.-L. Lee, and J. Zegenhagen, Phys. Rev. B **71**, 205425 (2005).
[49]Y. Zhang, S. Wang, T. Learmonth, L. Plucinski, A. Matsuura, S. Bernardis, C. O'Donnell, J. Downes, and K. Smith, Chem. Phys. Lett. **413**, 95–99 (2005).
[50]P. L. Cook, W. Yang, X. Liu, J. M. García-Lastra, A. Rubio, and F. J. Himpsel, J. Chem. Phys. **134**, 204707 (2011).
[51]W. Chen, D. C. Qi, Y. L. Huang, H. Huang, Y. Z. Wang, S. Chen, X. Y. Gao, and A. T. S. Wee, J. Phys. Chem. C **113**, 12832–12839 (2009).
[52]B.-E. Schuster, M. Benedetta Casu, I. Biswas, A. Hinderhofer, A. Gerlach, F. Schreiber, and T. Chassé, Phys. Chem. Chem. Phys. **11**, 9000–4 (2009).
[53]E. Salomon, N. Papageorgiou, T. Angot, A. Verdini, A. Cossaro, L. Floreano, A. Morgante, L. Giovanelli, and G. Le Lay, J. Phys. Chem. C **111**, 12467–12471 (2007).
[54]O. V. Molodtsova, M. Knupfer, V. V. Maslyuk, D. V. Vyalikh, V. M. Zhilin, Y. A. Ossipyan, T. Bredow, I. Mertig, and V. Y. Aristov, J. Chem. Phys. **129**, 154705 (2008).
[55]O. V. Molodtsova and M. Knupfer, J. Appl. Phys. **104**, 083704 (2008).
[56]S. Kera, M. B. Casu, A. Schöll, T. Schmidt, D. Batchelor, E. Rühl, and E. Umbach, J. Chem. Phys. **125**, 014705 (2006).
[57]F. Evangelista, V. Carravetta, G. Stefani, B. Jansik, M. Alagia, S. Stranges, and A. Ruocco, J. Chem. Phys. **126**, 124709 (2007).
[58]A. Nilsson, O. Björneholm, E. O. F. Zdansky, H. Tillborg, N. Mårtensson, J. N. Andersen, and R. Nyholm, Chem. Phys. Lett. **197**, 12–16 (1992).
[59]W. Wurth, D. Coulman, A. Puschmann, D. Menzel, and E. Umbach, Phys. Rev. B **41**, 12933–12936 (1990).
[60]O. V. Molodtsova, M. Knupfer, V. Yu. Aristov, D. V. Vyalikh, V. M. Zhilin, and Y. A. Ossipyan, J. Appl. Phys. **103**, 053711 (2008).
[61]V. Y. Aristov, O. V. Molodtsova, V. V. Maslyuk, D. V. Vyalikh, T. Bredow, I. Mertig, A. B. Preobrajenski, and M. Knupfer, Org. Electron. **11**, 1461–1468 (2010).
[62]V. Y. Aristov, O. V. Molodtsova, and M. Knupfer, Org. Electron. **12**, 372–375 (2011).
[63]I. Kröger, B. Stadtmüller, C. Stadler, J. Ziroff, M. Kochler, A. Stahl, F. Pollinger, T.-L. Lee, J. Zegenhagen, F. Reinert, and C. Kumpf, New J. Phys. **12**, 083038 (2010).
[64]M. P. de Jong, R. Friedlein, S. L. Sorensen, G. Öhrwall, W. Osikowicz, C. Tengsted, S. K. M. Jönsson, M. Fahlman, and W. R. Salaneck, Phys. Rev. B **72**, 035448 (2005).
[65]W. Eberhardt, Physica Scripta **T17**, 28–38 (1987).
[66]W. Eberhardt, J. Stöhr, D. Outka, and R. J. Madix, Solid State Commun. **54**, 493–496 (1985).
[67]N. Tsukahara, K.-I. Noto, M. Ohara, S. Shiraki, N. Takagi, Y. Takata, J. Miyawaki, M. Taguchi, A. Chainani, S. Shin, and M. Kawai, Phys. Rev. Lett. **102**, 167203 (2009).